



Elovl4 and *Fa2h* expression during rat spermatogenesis: a link to the very-long-chain PUFAs typical of germ cell sphingolipids^S

Florencia X. Santiago Valtierra,* Daniel A. Peñalva,* Jessica M. Luquez,* Natalia E. Furland,* Claudia Vásquez,[†] Juan G. Reyes,[†] Marta I. Aveldaño,* and Gerardo M. Oresti^{1,*}

Instituto de Investigaciones Bioquímicas de Bahía Blanca,* Consejo Nacional de Investigaciones Científicas y Técnicas (CONICET) y Universidad Nacional del Sur (UNS), Bahía Blanca, Argentina; and Instituto de Química,[†] Facultad de Ciencias, Pontificia Universidad Católica de Valparaíso, Valparaíso, Chile

Abstract The sphingolipids (SLs) of rodent spermatogenic cells (spermatocytes, spermatids) and spermatozoa contain nonhydroxylated and 2-hydroxylated versions of very-long-chain (C26–C32) PUFAs (n-V and h-V, respectively) not present in Sertoli cells (SCs). Here, we investigated the expression of selected fatty acid elongases [elongation of very-long-chain fatty acid protein (*Elovl*)], with a focus on *Elovl4*, and a fatty acid 2-hydroxylase (*Fa2h*) in rat testes with postnatal development and germ cell differentiation. Along with *Elovl5* and *Elovl2*, *Elovl4* was actively transcribed in the adult testis. *Elovl4* mRNA levels were high in immature testes and SCs, though the protein was absent. The *Elovl4* protein was a germ cell product. All cells under study elongated [³H]arachidonate to tetraenoic and pentaenoic C24 PUFA, but only germ cells produced C26–C32 PUFAs. Spermatocytes displayed the highest *Elovl4* protein levels and enzymatic activity. *Fa2h* mRNA was produced exclusively in germ cells, mostly round spermatids. As a protein, *Fa2h* was mainly concentrated in late spermatids, in the step of spermiogenesis in which they elongate and their heads change shape. The expression of *Elovl4* and *Fa2h* thus correlate with the abundance of n-Vs and h-Vs in the SLs of rat spermatocytes and spermatids, respectively.—Santiago Valtierra, F. X., D. A. Peñalva, J. M. Luquez, N. E. Furland, C. Vásquez, J. G. Reyes, M. I. Aveldaño, and G. M. Oresti. *Elovl4* and *Fa2h* expression during rat spermatogenesis: a link to the very-long-chain PUFAs typical of germ cell sphingolipids. *J. Lipid Res.* 2018. 59: 1175–1189.

Supplementary key words differentiation • elongation of very-long-chain fatty acid 2 • elongation of very-long-chain fatty acid 4 • elongation of very-long-chain fatty acid 5 • fatty acid 2-hydroxylase • Sertoli cells • spermatogenic cells

This work was supported by Agencia Nacional de Promoción de la Ciencia y la Tecnología Grant PICT2013-2533, Consejo Nacional de Investigaciones Científicas y Técnicas Grant PIP112-201101-00843, Secretaría General de Ciencia y Tecnología, Universidad Nacional del Sur Grant PGI 24/B218, Argentina, and Fondo Nacional de Desarrollo Científico y Tecnológico Grant 1140758, Chile. The authors declare no conflicts of interest with the contents of this article.

Manuscript received 12 November 2017 and in revised form 27 April 2018.

Published, *JLR Papers in Press*, May 3, 2018
DOI <https://doi.org/10.1194/jlr.M081885>

Very-long-chain PUFAs (VLCPUFAs) (C26–C32) of the n-6 series with four and five double bonds typically compose the sphingolipids (SLs) of rodent testes. These fatty acids occur in nonhydroxy-VLCPUFA (n-V) and 2-hydroxy-VLCPUFA (h-V) versions in SMs and ceramides (Cers) of spermatogenic cells and spermatozoa (1–4), and also in a germ cell-specific series of complex glycosphingolipids (5, 6). Deletion of different genes involved in the biosynthesis of these SLs results in impaired spermatogenesis (6, 7).

To produce VLCPUFAs, stepwise fatty acid elongation and desaturation reactions starting from C18 PUFAs are required to produce C20 and C22 tetraenoic, pentaenoic, or hexaenoic PUFAs, which can be further elongated to PUFAs with C24 and longer chains. Seven isoforms of fatty acid elongases are presently known, their substrate specificities tending to differ with chain length and unsaturation of the corresponding acyl-CoAs (8). Members of the elongation of very-long-chain fatty acid protein (*Elovl*) family of genes encode for enzymes embedded in the endoplasmic reticulum (ER) that are responsible for the rate-limiting condensation reaction that leads to the elongation of fatty acids (8). Among these, high mRNA levels of *Elovl5* and *Elovl2* have been found in the human and mouse testis (9), whose glycerophospholipids are known to be rich in C20 and C22 PUFAs of the n-6 and n-3 series. The *Elovl2*-derived

Abbreviations: *Agps*, alkylglycerone phosphate synthase; Cer, ceramide; CNRQ, calibrated normalized relative quantity; *Elovl*, elongation of very-long-chain fatty acid protein; ER, endoplasmic reticulum; *Fa2h*, fatty acid 2-hydroxylase; FAME, fatty acid methyl ester; *Hprt*, hypoxanthine-guanine phosphoribosyl transferase; h-V, 2-hydroxy-very-long-chain PUFA; LS, late spermatid; n-V, nonhydroxy-very-long-chain PUFA; *Pgk1*, phosphoglycerate kinase; PS, primary spermatocyte; PtS, pachytene spermatocyte; qPCR, quantitative PCR; RS, round spermatid; SC, Sertoli cell; SG, spermatogonia; SL, sphingolipid; ST, seminiferous tubule; *Tbp*, TATA box-binding protein; VLCPUFA, very-long-chain PUFA.

¹To whom correspondence should be addressed.

e-mail: gmoresti@criba.edu.ar

^SThe online version of this article (available at <http://www.jlr.org>) contains a supplement.

24:4n-6 and 24:5n-3 may be subject to $\Delta 6$ desaturation to produce 24:5n-6 and 24:6n-3, respectively, and these C24 PUFAs may be further elongated to give rise to several n-Vs, 30:5n-6 among others, in the mouse testis (10). Ablation of the *Elovl2* gene in mice results in deficiency from the testis of C24 and longer PUFAs, in association with arrested spermatogenesis (10).

In the retina of some vertebrates, PUFAs with chain lengths up to 34:5n-6 and 34:6n-3 also abound, highly concentrated in the phosphatidylcholine present in the rhodopsin-containing disk membranes of rod retinal photoreceptors (11, 12). *Elovl4*, the enzyme responsible for the synthesis of retinal VLCPUFAs, is encoded by the *Elovl4* gene. This concurs with the fact that the retina displays a high expression of this gene among primate (13) and mouse (14) tissues. From invertebrates to mammalian species, *Elovl4* orthologs share sequence homology with human *ELOVL4*, suggesting functional conservation during evolution (15). The human *ELOVL4* gene and the protein it encodes have received intense research because specific mutations in the human *ELOVL4* gene are associated with different forms of retinal macular dystrophies that include Stargardt disease type 3 (15–19), a group of blindness-causing disorders. Using a gain-of-function approach in cells in culture (20) and photoreceptor-specific conditional knockout mice (21), direct evidence was provided that *Elovl4* is required for the biosynthesis of the VLCPUFAs typical of retina (20, 21) and for proper photoreceptor function (21). Considering that in addition to sharing the type of VLCPUFAs produced, mouse retina and testes share an important expression of the *Elovl4* gene (14), it is not unlikely that ablation or mutations in this gene will affect male fertility.

In testes from immature rats, Cer and SM do not contain PUFAs longer than C24. The proportion of n-Vs increases concomitantly with the appearance of the first round of pachytene spermatocytes (PtSs) and that of h-Vs accompanies that of spermatids (4). The h-V-containing species of Cer and SM may be considered a hallmark of germ cell differentiation, as their concentrations increase from round spermatids (RSs) to elongated spermatids [late spermatids (LSs)] to finally become components of spermatozoa (3, 22). The biosynthesis of these fatty acids is expected to require the activity of a fatty acid 2-hydroxylase (*Fa2h*).

The *Fa2h* gene is highly expressed in mammalian brain (23, 24) and peripheral nerve (25) and also in skin (26, 27), where it is thought to encode the enzyme responsible for the 2-hydroxylation of the very-long-chain (saturated) fatty acids that abound in myelin galactosylceramides and skin glucosylceramides. In addition to brain, skin, and intestine, the mouse homolog of *Fa2h* is markedly expressed in adult testes (23), where it may encode the form of *Fa2h* that is responsible for the abundance of h-Vs in rodent spermatogenic cell SLs.

In the present study, the seven *Elovl* family members were investigated for their transcription (mRNA) in adult rat testes. A special emphasis was given to *Elovl4*, on the assumption that the *Elovl4* enzyme participates in the biosynthesis of n-Vs. *Elovl5* and *Elovl2* were included in this context because the enzymes they code cooperate in the

elongation of C18–C24 PUFAs, thus playing important roles as providers of the major C20 and C22 PUFAs of testis on the one hand, and as providers of the C24 PUFAs that will then be further elongated by *Elovl4* on the other. The postnatal developmental and cell type-associated transcription levels of the three *Elovl* genes are compared, and their concurrent activity as enzymes is shown to be maximal in PtSs, decreasing in spermatogenic cells as they mature. *Elovl4* and *Fa2h* are shown to be transcribed and translated differentially during testicular development and to arise at differentiation stages and cell locations that correlate with the abundance of membrane SLs with n-Vs and h-Vs in spermatocytes and spermatids, respectively.

MATERIALS AND METHODS

Tissue and cell isolation

Male Wistar rats of different ages were used. The animals, housed in a standard animal facility kept at 22°C, 50–55% humidity, and 12:12 h light:dark cycles, were allowed ad libitum access to food and water. The experimental protocols were approved by the institutional Committee for the Care and Use of Laboratory Animals of the Universidad Nacional del Sur, Argentina. Whole testes were obtained at the postnatal days indicated in the Results, from postnatal day (P)14 to P90 (adult) males. Seminiferous tubules (STs) were isolated from adult testes and, after enzymatic digestion with collagenase, trypsin, and DNase, the resulting germ cell suspensions were subjected to velocity sedimentation separation through BSA density gradients by the STAPUT technique (28). Fractions containing PtSs, RSs, and LSs were obtained and identified as previously described (3, 29). As an average, these preparations showed respective purities of 84, 90, and 76%. To ensure absence of germ cells from Sertoli cell (SC) preparations, the latter were obtained from prepubertal testes (rats aged 14–16 days) following standard procedures (30) and cultured during 2 weeks at 37°C under a 5% CO₂/95% air atmosphere in DMEM:F12 serum-free medium (Gibco, BRL; 1:1, v/v) before use.

*Elovl*s and *Fa2h* mRNA

*RT-PCR of Elovl*s mRNAs. The RNA from testes, STs, and cell preparations was isolated using TRIzol reagent (Invitrogen, Carlsbad, CA) according to the manufacturer's instructions. Total RNA samples were suspended in RNase-free water, their quality and concentrations were assessed using a PicoDrop spectrophotometer, and they were stored at –80°C until use. From the 260/280 absorbance ratios, the RNA purity ranged from 1.75 to 1.95 (mean 1.85). Total RNA (2 µg) was used to synthesize cDNA by reverse transcription in a final volume of 25 µl. The reverse transcription reaction vials contained 1 µg Random Primers hexamers (Biodynamics), 1× M-MLV RT reaction buffer, 0.5 mM each of dNTP, 25 UI RNase inhibitor (Promega), and 200 UI M-MLV RT (Promega). Of the cDNA solution, 3 µl were used for the PCR reaction with Taq DNA polymerase, carried out in a volume of 20 µl. The gene-specific primer pairs designed for the amplification of rat *Elovl*s (*Elovl1* to *Elovl7*) are listed in **Table 1**. Samples were denatured at 94°C for 5 min, followed by amplification rounds consisting of denaturation at 94°C for 30 s, annealing at specific temperature depending of the primer pair for 30 s, and final extension steps at 72°C, first for 30 s for 30 cycles and then for 10 min. The RT-PCR products were stained with ethidium bromide and assessed using 1.5% agarose gel electrophoresis.

TABLE 1. Sequences of the primer pairs used and size of the fragments produced by normal and quantitative RT-PCR

Genes	Primer Sequences (5'-3')	Aim	Amplicon Lengths (nt)	Efficiency (%)	Annealing Temperature (°C)
<i>Elovl1</i>	F: CTCACTGCACATCAGCCAATA R: GAGTCTGGTCATGGGTGTAG	RT-PCR	301		57.5
<i>Elovl2</i>	F: CAGCACACAGGCACCAGG R: GACTTCAGTGGCTCTCACGG	RT-PCR	568		57.5
<i>Elovl3</i>	F: CAAAGTGAAGCATCCCAACAT R: GGTTGTCATAGCTTCCTGCAA	RT-PCR	384		54
<i>Elovl4</i>	F: GGTTGAGTTCCATGTGACCAT R: TCTGTTGCCCTGAACTTTTA	RT-PCR	346		56
<i>Elovl5</i>	F: ACCACCATGCCACTATGCT R: GTGTCCATTGACGGCAGT	RT-PCR	407		55
<i>Elovl6</i>	F: GCTGATCTTCCTGCACTGGTA R: CGTGATGACCCTGAGCTATGT	RT-PCR	438		57.5
<i>Elovl7</i>	F: GGGACCAGCCTACCAGAAGTA R: TCAAGGAAGGCAAGATAGCAG	RT-PCR	321		57.5
<i>β-Actin</i>	F: ATGGATGACGATATCGCTG R: ATGAGGTAGTCTGTGAGG	RT-PCR	569		58
<i>Elovl2</i>	F: CGGAATCACACTTCTTTCTGC R: CACTGCAAGTTGTAGCCTCCT	RT-qPCR	78	107.2	58
<i>Elovl4</i>	F: GGTGGATTGGAATCAAGTGG R: TACCGCTTCCACCAAAGGTA	RT-qPCR	145	104.4	58
<i>Elovl5</i>	F: GAGGCATCCTGGTGGTGTAT R: ACACACCTGTCACCAACTCATAG	RT-qPCR	78	110.3	58
<i>Fa2h</i>	F: AGTACTATGTGGGCGAACTGC R: CAATAGCAGCATCTGTCTTCTGA	RT-qPCR	96	105.4	58
<i>β-Actin</i>	F: AAGGCCAACCCTGAAAAGAT R: ACCAGAGGCATACAGGGACA	RT-qPCR	102	109.2	58
<i>Agps</i>	F: CCGAGTACCAATGAGTGCAA R: CCATCCATTCCATTTCATAAGTT	RT-qPCR	132	110.4	58
<i>Hprt</i>	F: CTCATGGACTGATTATGGACAGGAC R: GCAGGTCAGCAAAGAAGCTATAGCC	RT-qPCR	123	110.5	58
<i>Pgk1</i>	F: GCAAAGACTGGCCAAGCTAC R: GCCTCAGCATATTTCTTACTGCT	RT-qPCR	95	108.7	58
<i>Tbp</i>	F: TGGGATTGTACCACAGCTCCA R: CTCATGATGACTGCAGCAAACC	RT-qPCR	132	104.7	58

F, forward; R, reverse.

Quantitative PCR for *Elovl5*, *Elovl2*, *Elovl4*, and *Fa2h*. The cDNAs were amplified by real-time quantitative PCR (qPCR) in a final reaction volume of 10 μ l using KAPA SYBR FAST Master Mix (Kapa Biosystems) and a 0.20 μ M concentration of each primer. Primer sequences for the specific amplification of rat *Elovl2*, *Elovl5*, *Elovl4*, and *Fa2h* genes (Table 1) were designed with Primer3 software and purchased from Invitrogen Life Technologies. Gene expression levels and melt-curve analyses were determined using Rotor-Gene 6000 (Corbett Research, Australia). The PCR conditions were as follows: 40 cycles of denaturation at 94°C for 20 s, annealing and extension at 58°C for 30 s, and a final extension step at 72°C for 30 s. The PCR products were confirmed by agarose gel electrophoresis (supplemental Fig. S1).

Data analysis and validation. In each physiological or experimental condition (developmental stage, cell type, or weeks after hyperthermia treatment) a total of 12 measurements for each gene under study were performed: three biological replicates (three independent reverse transcription reactions) and four technical replicates. Using a pool of cDNA from all experimental conditions, standard curves using 1/10 dilution series were prepared and the amplification efficiencies of target and reference genes were calculated, which ranged between 104% and 110% (Table 1).

For normalization of data against validated reference genes, the raw Cq values of the target genes (*Elovl5*, *Elovl2*, *Elovl4*, and *Fa2h*) and the following five candidates to reference genes: β -Actin, alkylglycerone phosphate synthase (*Agps*), hypoxanthine-guanine phosphoribosyl transferase (*Hprt*), TATA box-binding

protein (*Tbp*), and phosphoglycerate kinase (*Pgk1*) were imported into the qBasePLUS software (31). In qBasePLUS, the geNorm module was used to identify the most stable reference gene combination for each experiment (32). In the case of data sets from postnatal development and posthyperthermia treatment samples, the combination of five genes (β -Actin, *Agps*, *Hprt*, *Tbp*, and *Pgk1*) gave a reference gene stability factor (geNorm M) of 0.47 and 0.24 (optimal <0.5) and a variability between sequential normalization factors (geNorm V) of 0.15 and 0.15 (preferable <0.15), respectively. In the case of data sets from isolated cell types (SCs, PtSs, RSs, and LSs), quality analysis (qBasePLUS) indicated that inclusion of β -Actin and *Tbp* reduced reference gene stability when comparing expression levels on the different cell types under study. For this reason, β -Actin and *Tbp* were omitted as reference genes, and the combination of three reference genes (*Agps*, *Hprt*, and *Pgk1*) was found to be optimal to compare the expression of the three elongases and *Fa2h*, as this combination produced a good M value and the lowest V factor. Using the reliable and validated reference gene combination for each sample, the reported levels of *Elovl5*, *Elovl2*, *Elovl4*, and *Fa2h* were calculated as calibrated normalized relative quantity (CNRQ) values. These values were then exported from the qBasePLUS software and statistically investigated.

***Elovl5*, *Elovl2*, *Elovl4*, and *Fa2h* mRNA in the adult testis.** The mRNA transcribed from each gene in vivo was evaluated simultaneously in the testis of adult rats. Untreated animals, used as controls, were compared with counterparts experimentally deprived of spermatogenic cells. To generate “germ cell-free” testes in vivo,

3-month-old males were exposed to mild hyperthermia (33). In sedated rats, the caudal segment of the body was immersed into a water bath at 43°C for 15 min, once a day for five consecutive days. Control animals were subjected to the same procedures, except for the bath temperature (22–25°C). All animals were euthanized 2 and 6 weeks after the last of these exposures and their testes were removed. Part of them were fixed in 10% formaldehyde, embedded in paraffin, and cut into 3 µm sections for histological observation after hematoxylin-eosin staining, and part of them were subjected to RNA extraction and quantification to determine *Elovl5*, *Elovl2*, *Elovl4*, and *Fa2h* mRNA transcript levels.

Elovl4 and Fa2h proteins

Protein levels in tissue and cell samples were assessed by Western blot analysis. Immediately after isolation, homogenization was performed using lysis buffer [20 mM Tris-HCl (pH 7.4), 100 mM NaCl, 1 mM EDTA, complete protease inhibitor (Sigma P-8340)] and 1% Triton X-100. Aliquots were taken for protein quantification (DC Protein Assay; BIO-RAD Life Science Group, FL). Protein homogenates were dissolved in denaturing Laemmli buffer, boiled for 5 min (34), and resolved by SDS-PAGE on 10% polyacrylamide gels, loading equivalent amounts of protein (30 µg) per lane. After electrophoresis, proteins were electroblotted to PVDF membranes (Millipore, Bedford, MA) and blocked with 5% BSA in TBS-T buffer [20 mM Tris-HCl (pH 7.4), 100 mM NaCl, and 0.1% (w/v) Tween 20] for 2 h at room temperature. The PVDF membranes were incubated overnight at 4°C with the primary rabbit polyclonal antibody, either against Elovl4 (1:1,000 in BSA) or Fa2h (1:500 in BSA). For Elovl4, a rabbit anti-Elovl4 antibody was used, kindly donated by Dr. Robert E. Anderson (University of Oklahoma Health Sciences Center, Oklahoma City, OK), previously validated for Western blot and immunohistochemistry (20). For Fa2h, the antibody, ab111554 anti-Fa2h, from Abcam was employed. After primary antibody contact, samples were exposed for 2 h at room temperature with HRP-conjugated goat anti-rabbit secondary antibody (sc-20049; Santa Cruz Biotechnology) (1:2,000). The membranes were then washed with TBS-T buffer and the immunoreactive bands were detected by ECL (Amersham Biosciences) using standard X-ray films (Kodak X-Omat AR). For loading control, the PVDF membranes were reprobed with a mouse anti-α tubulin antibody (1:4,000; DM1-A) (CP06; EMD/Biosciences-Calbiochem) for 3 h and with the corresponding HRP-labeled goat anti-mouse secondary antibody (1:2,000; sc-2005 from Santa Cruz Biotechnology). Protein band intensities were compared using the ImageJ software (National Institutes of Health, Bethesda, MD).

Elovl activity

For detection of long and very-long PUFAs synthesized by the coordinated activity of the Elovls under study, the transformations undergone by [³H]20:4n-6 as precursor were followed. STs, the germ cells isolated therefrom, and SCs prepared as described above, were separately placed in 35 mm diameter dishes suspended in the culture medium. The [³H]20:4n-6 was added and cultures proceeded for 20 h at 32°C in a tissue culture incubator under 5% CO₂/95% air and 95% relative humidity. The medium was DMEM without glucose (Gibco, BRL, Grand Island, NY), supplemented with 5% (v/v) FBS, 6 mM lactate, penicillin (100 U/ml), and streptomycin (100 U/ml). In a final volume of 2 ml of medium, an amount of STs equivalent to 1.5 mg of protein and an amount of cells adjusted to contain 5 × 10⁶ cells per plate were used. Incubations started with the addition of 1 µCi of [³H]20:4n-6 (65.9 Ci/mmol; Perkin Elmer Life Sciences Inc., Boston, MA), previously diluted with unlabeled 20:4n-6 to reach a 2.5 µM final concentration. Tubules and cells were then transferred to glass tubes, separated from the [³H]labeled media by centrifugation (at 800 g for

5 min), and washed twice by suspension in PBS and similar centrifugations. The materials in the sediments were recovered for lipid extraction (35). After partitions and washings of the extracts, the total lipid was dried under N₂ and dissolved in chloroform-methanol. Aliquots from these lipid extracts were taken to check the incorporation of label from [³H]20:4 into lipids and its distribution among lipid classes. After separating the major classes by TLC, most of the label was found to be esterified into lipids, the fraction remaining as free fatty acid varying among PtSs and RSs (supplemental Fig. S2). With no remarkable differences among cells, most of the esterified label was distributed between polar (choline-, ethanolamine-, and inositol-glycerophospholipids) and nonpolar lipids (mainly triacylglycerols).

To explore the transformations undergone by [³H]20:4 into longer and more unsaturated PUFAs after the described 20 h incubations, the [³H]labeled fatty acids from the total lipid extracts of STs and cells were examined. Fractions from these extracts were converted into fatty acid methyl esters (FAMEs), which were then separated according to unsaturation and chain length by a combination of argentation TLC and reverse phase HPLC.

To prepare FAMEs, the classical procedure described by Christie (36) was used. Fractions from the total lipid samples were placed into glass tubes fitted with screw caps and the solvents evaporated under N₂. Nitrogen-saturated, dehydrated methanol-H₂SO₄ was then added and, after adding a N₂ gas atmosphere, the tubes were closed and kept at 45°C overnight. The resulting FAMEs were recovered into hexane after adding water and hexane to the methanol solution, mixing thoroughly, and recovering the upper hexane phases. The FAME preparations were subjected to TLC for recovery of (nonhydroxy and 2-hydroxy) FAMEs. Pre-washed silica gel G plates and two proportions of hexane:ether were used. The first one (80:20 v/v) was run up to the middle of the plates, and the second one (95:5 v/v) up to near the top (4, 37). After location, FAMEs and 2-hydroxy-FAME bands were eluted by thoroughly mixing them with water:methanol:hexane (1:1:1 v/v), recovering the hexane layer, and carrying out two additional hexane extractions. The bulk of the [³H]radioactivity appeared in the nonhydroxy-FAME fraction, whereas the one containing 2-hydroxy-FAME was devoid of detectable label.

To separate the total [³H]labeled FAME in samples according to unsaturation, TLC plates prepared with silica gel G and 20% w/w AgNO₃ as support and chloroform:methanol (90:10 v/v) as solvent were used. The bands containing the [³H]labeled tetraenoic and pentaenoic FAME fractions were recovered and eluted as just described. The eluate volumes were reduced under N₂, filtered to remove traces of particulate matter, dried under N₂, and dissolved in methanol. The components of each of the two fractions were then separated according to chain length by HPLC, using an Eclipse Plus HPLC column (Agilent Technologies) kept at 40°C and acetonitrile:water (98:2 v/v) at a flowrate of 0.75 ml/min. The (100 × 4.6 mm) column contained 3.5 µm spherical particles covered with octadecylsilane. The polyunsaturated FAMEs were detected by their absorbance at 203 nm and collected as they emerged from the column. After evaporating the solvents, the collected compounds were transferred to vials and their [³H]label was measured by liquid scintillation counting.

Immunohistochemistry

Immunochemical staining with labeled antibodies against Elovl4 and Fa2h was used for selectively imaging these proteins in testis sections. Retina and brain tissue had been previously used as positive controls to set the assays for Elovl4 (1:100 in PBS with 2% BSA) and Fa2h (1:50 in PBS with 2% BSA), respectively. Samples containing BSA and no primary antibody were used as negative controls (see supplemental Fig. S3). Rat testes were fixed by immersion in 4% paraformaldehyde overnight at 4°C, rinsed in a

graded series of sucrose concentrations (10 to 20 to 30%) in PBS at 4°C for cryoprotection, embedded in a small amount of OCT compound Tissue Tek (Sakura Finetek, Torrance, CA), and stored at -80°C. Frozen 5–7 μm thick sections were prepared using a cryostat (Leica CM 1860), picked up on SuperFrost Plus slides (Thermo Scientific), and refrigerated until stained. Then, tissue sections were incubated in PBS to remove OCT and postfixed for 2 min in 4% paraformaldehyde. The latter had been dissolved in PBS or in acetone:methanol (1:1), if destined to Elov14 or to Fa2h immunodetection, respectively. Fixed tissue sections were washed with PBS and permeabilized with 0.1% Triton X-100 (Sigma-Aldrich) in PBS for 10 min at room temperature. After washing, the sections were blocked with 2% BSA in PBS for 20 min and incubated overnight at 4°C with the corresponding antibody. After extensive washing with PBS, the tissue sections were incubated for 1 h at room temperature with the corresponding secondary goat anti-rabbit antibodies, conjugated with Alexa Fluor 568 in the case of Elov14 and with the 488 dye (Life Technologies) in the case of Fa2h (1:500 in PBS with 2% BSA). For cell nuclei location, the tissue sections were incubated with a 5 μM solution of Hoechst 33342 or TO-PRO in PBS for 10 min, briefly washed with PBS, and mounted with Fluoromount™ aqueous mounting medium (Sigma, St. Louis, MO). All stained sections were observed under a Nikon Eclipse E-600 fluorescence microscope equipped with a 40× NA 1.0 oil-immersion objective. Images were captured and processed using a model ST-7 SBIG CCD camera driven by the CCDOPS software, version 5.02 (SBIG Astronomical Instruments). The micrographs shown in the Results are representative of experiments repeated at least four times by two different investigators using samples from different rats, with similar results. A confocal laser scanning microscope (Leica DMIRE2) was used to get details of intracellular Elov14 and Fa2h localization in immunostained tissue sections.

Statistical analysis

One-way ANOVA was used to determine differences among mean values, which were compared using Tukey's multiple comparison test. Data in the figures are presented as mean values ± standard deviation from at least three individual samples, obtained from independent tissue and cell preparations.

RESULTS

Expression of *Elovl* family genes

In previous work the mRNA of two enzymes involved in PUFA elongation, *Elovl5* and *Elovl2*, were shown to be expressed in rat germ cells at two stages of cell differentiation: PtS and RS (3). Here we extended the study, using RT-PCR analysis, to other cells from the seminiferous epithelium and to other known members of the *Elovl* family (Fig. 1). Of the seven mammalian *Elovl* family members explored, except *Elovl3*, the transcripts of six isoforms were detected in cells located within STs (Fig. 1). In semi-quantitative terms, the most abundant transcript in SCs was that of *Elovl6* and, albeit faintly, the *Elovl7* mRNA was detected only in these cells. The mRNAs of *Elovl1*, *Elovl2*, *Elovl5*, *Elovl6*, and *Elovl4* were actively expressed in germ cells (PtSs and RSs) as well as in SCs.

Elovl5, *Elovl2*, and *Elovl4* mRNA expression

Given the collaborative activities of *Elovl5* and *Elovl2* to produce the elongated PUFAs that serve as substrates of

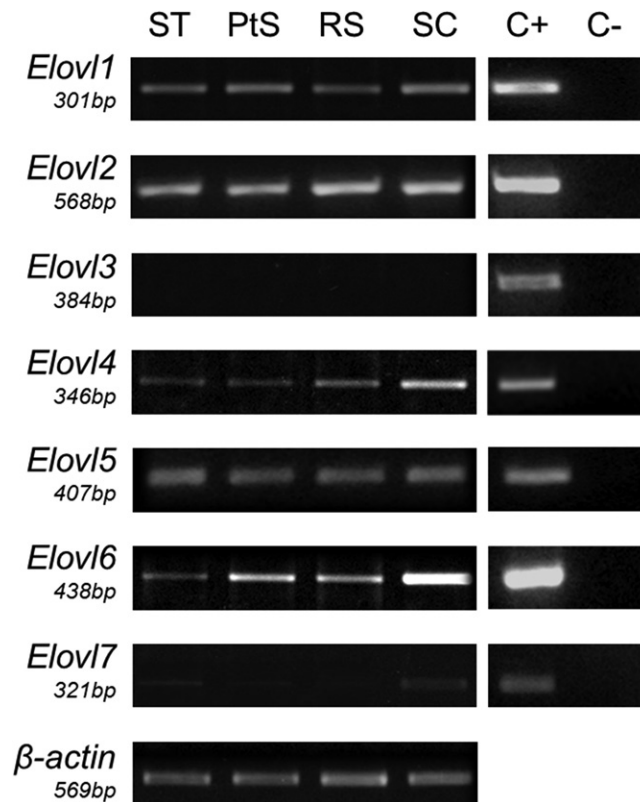


Fig. 1. PCR analyses of *Elovl* family member transcripts in adult rat STs and in cell populations isolated therefrom. Positive controls (C+), shown for comparison, contained total RNA from liver (for *Elovl1*, *Elovl2*, *Elovl5*, and *Elovl6*), brown adipose tissue (*Elovl3*), retina (*Elovl4*), and adrenal gland (*Elovl7*). Negative controls (C-) included RNase-free water instead of cDNA in the amplification reactions.

Elovl4, and the expected association of the latter with the n-Vs of rat spermatogenic cells, we followed by RT-qPCR their expression patterns through the postnatal period and during germ cell differentiation (Fig. 2). The expression level of *Elovl5* was relatively stable from prepubertal ages (P14) to adulthood in testes. Among germ cells, *Elovl5* showed far higher levels of expression by the two spermatids than by PtSs. *Elovl5* mRNA levels in the latter were similar to those in SCs.

Unlike *Elovl5*, the *Elovl2* mRNA levels were very low at early developmental stages (P14). They augmented significantly at P21 and P25, in coincidence with the appearance of the first generation of spermatocytes (PtSs), and showed an evident upsurge from P25 to P30, concurrently with the timing of appearance in the testis of the first generation of spermatids, to remain high from this age to adulthood (Fig. 2). Among seminiferous epithelium cell types, *Elovl2* was strongly expressed in all three spermatogenic cell types studied. Albeit not negligible (Cq value: 24), its expression was lower in SCs than in germ cells.

The *Elovl4* mRNA levels in rat testes, against our expectations, were the highest at infantile ages (P14) (Fig. 2). They decreased significantly toward juvenile ages (P25) and, although more slowly, continued to decrease during the postpubertal period (P45). From this moment onwards,

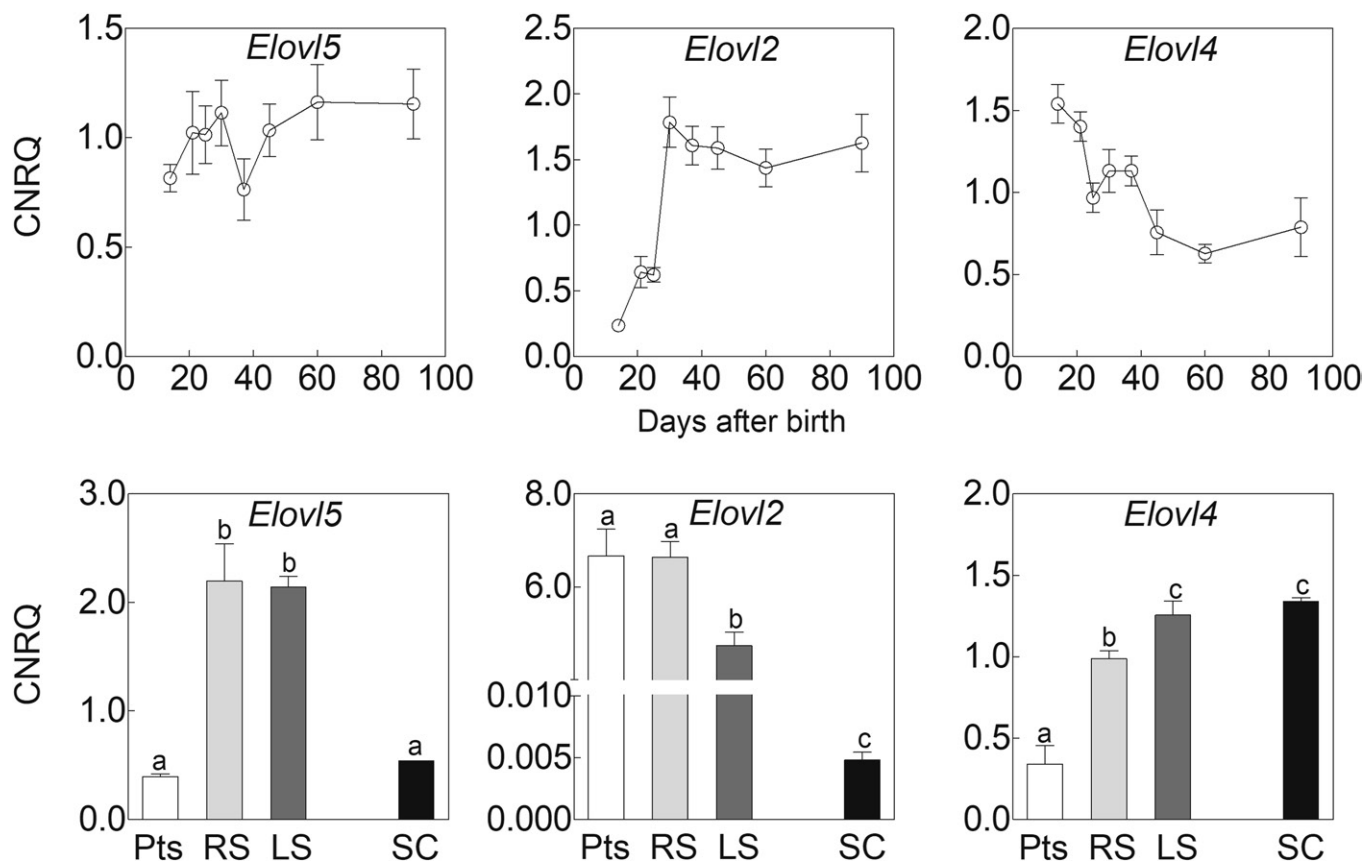


Fig. 2. RT-qPCR analyses of *Elov15*, *Elov2*, and *Elov4* transcripts in rat testis during postnatal development and in cell types from adult rat STs. The data are shown as normalized relative expression values in arbitrary units (CNRQ \pm SEM), determined as described in the Materials and Methods. Values with different letters (a–c) represent significant differences among cells ($P < 0.05$).

the mRNA levels plateaued, remaining in the relatively stable levels typical of adulthood (P90).

The distribution of *Elov4* mRNA among cells of the seminiferous epithelium explained the high expression of this gene observed at P14, taking into account that, at that age, the seminiferous epithelium is mainly composed of SCs (65% of the testicular cells). Thus, *Elov4* transcript levels were remarkably high in these somatic cells (Fig. 2). Because they were obtained from P14 testes and cultivated for as long as 2 weeks with periodic changes of culture medium before the mRNA measurements, and considering that these cells display an inherent phagocytic activity, the probability is low that such mRNA would belong to spermatogonia (SG) or other cells contaminating the samples. The high *Elov4* mRNA levels in the present SC preparations may thus be considered constitutive.

Among adult spermatogenic cells, levels of the *Elov4* mRNA were lower in the meiotic PtSs than in the more differentiated RSs and LSs (Fig. 2).

Fa2h mRNA expression

The transcription of the *Fa2h* gene clearly differed from that of *Elov4* during postnatal testicular development, as shown by RT-qPCR (Fig. 3). Thus, *Fa2h* mRNA levels were undetectable in testes up to P25, augmented rapidly from P25 to P30, in coincidence with the appearance of RSs, and showed an even steeper increase from P30 to P35, in

coincidence with the timing of appearance of the first elongating spermatids. After this peak, the mRNA levels underwent a temporary, but significant, decrease from P35 to P45, and a less steep, but steady, increase thereafter up to adulthood (P90).

Unlike the high levels of *Elov4* mRNA, the *Fa2h* mRNA was absent altogether from SCs (Fig. 3). Among spermatogenic cells, the mRNA levels of *Fa2h* were lower in PtSs than in the two spermatids, being the highest in RSs.

Elongases and *Fa2h* mRNA levels and germ cell depletion

Short exposures of the testis of adult rats to mild hyperthermia, repeated once a day for 5 days, results in a significant loss of spermatogenic cells with permanence of SCs (33). Albeit affected in some of their functions, the latter cells remain viable (38) and, 12 weeks thereafter, the spermatogenic cells are mostly recovered. As an indirect means of exploring whether the high *Elov4* mRNA levels observed in immature SCs were also a feature of those from the adult testes, we followed the changes in gene expression of *Elov4* in comparison with those of *Elov15*, *Elov2*, and *Fa2h* in testes after exposures to hyperthermia, in comparison with untreated controls (Fig. 4). Two weeks after such exposures, and concomitantly with the depletion of spermatogenic cells with permanence of the hyperthermia-resistant somatic SCs and SG within tubules, *Elov2* mRNA levels decreased significantly and the *Fa2h* mRNA expression was

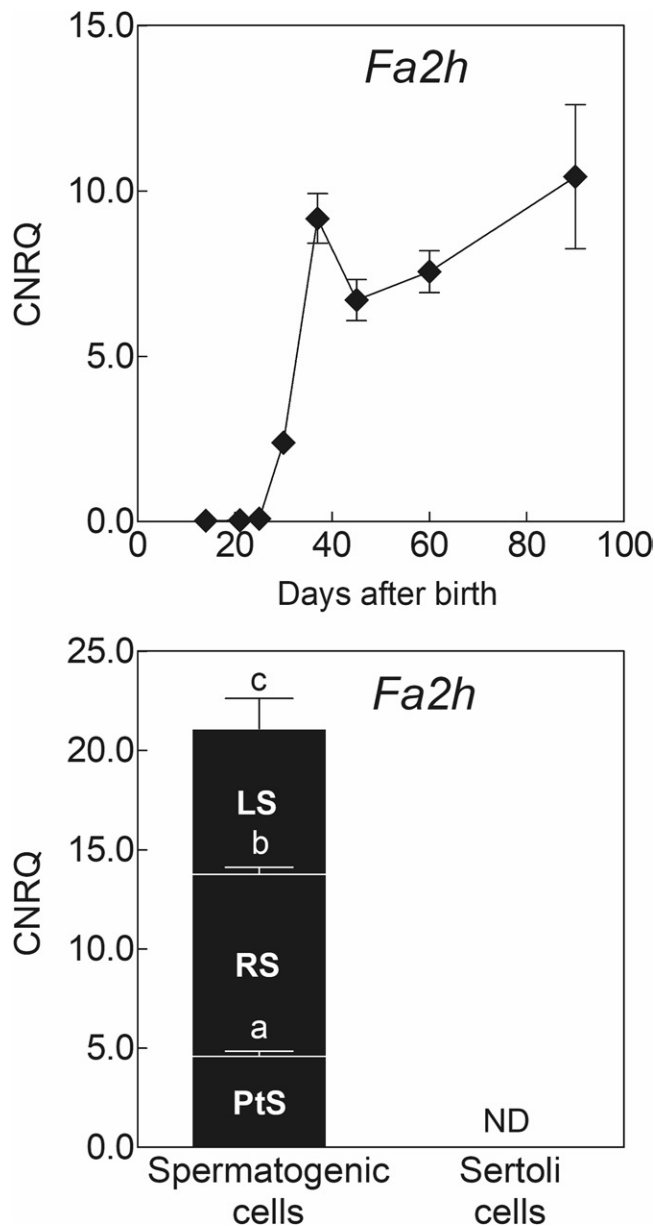


Fig. 3. RT-qPCR analyses of *Fa2h* transcript in rat testis during postnatal development and in cell types from adult rat STs. ND, not detected. The data are shown as normalized relative expression values in arbitrary units (CNRQ \pm SEM) determined as detailed in the Materials and Methods. Values with different letters (a–c) represent significant differences between cell types ($P < 0.05$).

virtually lost. Interestingly, *Elovl5* transcript levels markedly increased at the same time point. Those of *Elovl4* showed a similar trend of increase, although not significantly.

Six weeks after the heat exposures, the seminiferous epithelium had started to be repopulated with spermatogenic cells. Consistently, this was accompanied by the return to the control levels of *Elovl5* and *Elovl4* mRNA levels and a significant partial recovery of those of *Elovl2* and *Fa2h*. Resembling the tendency during postnatal development, as both situations encompass a change from a “mostly Sertoli” to a “mostly spermatogenic” cell-rich tissue, the relative *Elovl2* mRNA levels tended to increase, while those of *Elovl4* tended to decrease, from week 2 to week 6 posthyperthermia.

Elovl4 protein expression

In contrast to the high mRNA levels from *Elovl4*, the Elovl4 protein was absent from testes at early stages of testicular development (P14), when the STs are populated by proliferating SG and SCs (Fig. 5). Elovl4 was detected in Western blots at P21, reached a high expression at P25 (PtSs already present), and persisted at similar levels from P37 onwards (Fig. 5A). The distribution of Elovl4 among isolated cell populations complemented these observations by showing that the protein was absent altogether from SCs (Fig. 5A), while its levels were high in PtSs, RSs, and LSs. The time of appearance in the testis and the abundance among germ cells was confirmed in testicular tissue sections (Fig. 5B). Thus, the protein was immunodetected intensely at P21, in coincidence with the start of the pachytene phase of meiosis undergone by the first round of primary spermatocytes (PSs). These were virtually the only members of the spermatogenic cell line that were labeled at this developmental time point. SG and SCs, detected by the single row of close nuclei forming a layer adjacent to the basal membrane of the tubules, were unstained. The Elovl4 protein continued to be detected in differentiating germ cells from this age to adulthood. In different sections of the adult seminiferous epithelium the Elovl4 staining was concentrated in adluminal PSs, it was paler in the population of spermatids located above them (mainly RSs), and became bright-red again in elongating (early and late) spermatids close to the tubular lumen (Fig. 6), strongly condensed in small spot-like structures located in the areas close to tubular lumen. Interestingly, the staining of Elovl4 varied with the stage of the spermatogenic cycle (Fig. 6A). Thus, the staining in PtSs was the most intense among tubule cells at stages II–IV and VII–VIII, but became paler to the point of virtually fading in PtSs at stages V–VI, IX–XI, and XII–XIV (a scheme illustrating the stages accompanies Fig. 6B). This suggests that the enzyme concentration per cell decreases in PtSs in the last period of the long meiotic phase.

The Elovl4 localization was cytoplasmic in PtSs, and restricted to the perinuclear area, as expected for an ER-located enzyme (Fig. 6C). In PtSs and also in RSs, a higher concentration of the protein was observed in a distinctly perinuclear and more condensed structure. In elongating spermatids, Elovl4 was even more highly concentrated in a form of densely packed structure with an unspecified cytoplasmic localization that could correspond to the cytoplasmic lobe of spermatids.

Elovl5, Elovl2, and Elovl4 enzymatic activity

As a complement to their expression, the activity of elongases as enzymes was explored. Previous work showed that Elovl5 displays elongase activity with C18 and C20 PUFAs, but not C22 PUFAs, and that Elovl2 has lower activity with C18 PUFAs than with C20–C22 PUFAs (39), albeit C20 PUFAs (20:5n-3, 20:4n-6) are similarly good substrates for the two elongases (40). When [^3H]20:4n-6 was used as a substrate, ST segments and cells isolated therefrom clearly elongated it to 22:4 and further to 24:4, an anticipated function of Elovl5 and Elovl2 (Fig. 7). This activity was shared by SCs and germ cells.

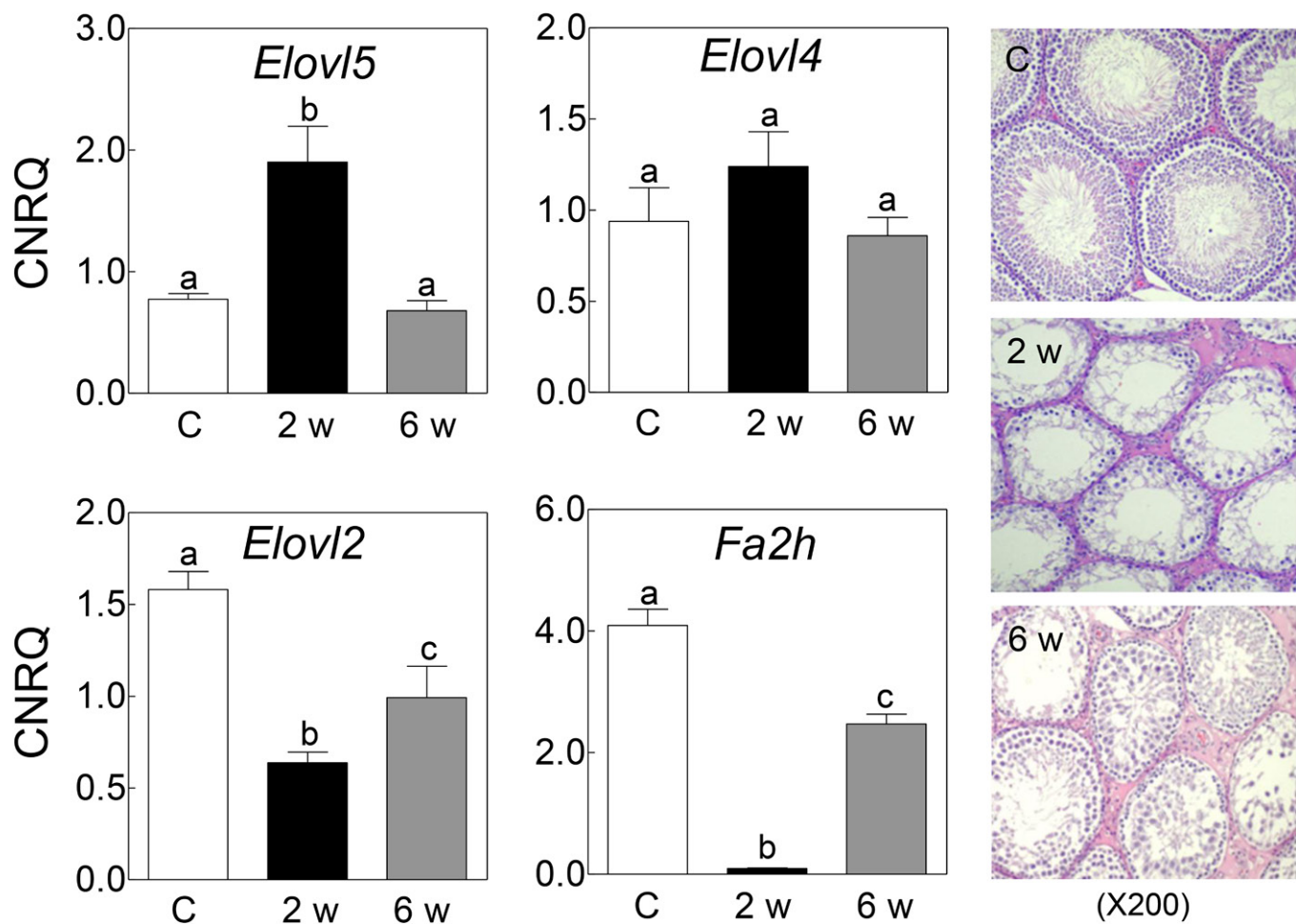


Fig. 4. Differential effects of the loss of spermatogenic cells from adult rat testes in vivo on the expression of *Elov15*, *Elov12*, *Elov4*, and *Fa2h*. Figures on the left show RT-qPCR analyses of transcripts in control (C) testes in comparison with testes that had been exposed once a day during 5 days to short episodes of mild hyperthermia and analyzed 2 and 6 weeks thereafter (2 w and 6 w, respectively). The data are shown as normalized relative expression values, in arbitrary units (CNRQ \pm SEM) determined as detailed in the Materials and Methods. Values with different letters (a–c) denote significant differences ($P < 0.05$). Figures on the right illustrate histological sections of the testes. At week 2, the STs were deprived of most mature spermatogenic cells, with SG and SCs remaining in the tubule lumina, while at week 6 a partial recovery of the seminiferous epithelium had started.

In consistency with their lack of *Elov4* protein, SCs did not produce quantifiable amounts of PUFAs longer than C24. Only in germ cells, significant proportions of the label appeared in longer tetraenes up to 28:4, as expected for a functional *Elov4* enzyme using the available [^3H]24:4 as its substrate (Fig. 7). Among the cells surveyed, and on the basis of a fixed amount of protein, PtSs showed the highest ability to produce C22–C24 PUFAs (22:4n-6 and 24:4n-6). As judged from the production of labeled tetraenoic n-Vs with C26–C32 chains, these cells also exhibited the highest *Elov4* activity.

An important proportion of the label from [^3H]20:4n-6 appeared in longer pentaenoic fatty acids, mostly [^3H]22:5n-6 and [^3H]24:5n-6 (Fig. 7). The formation of these two pentaenes manifests the presence of highly active desaturases in all seminiferous epithelium cells under study, including SCs. However, only in spermatogenic cells, the expected substrates of *Elov4*, [^3H]24:4, and [^3H]24:5, were further elongated to labeled tetraenes up to C28 and labeled pentaenes up to C32, respectively. The ratio (sum of [^3H]label

in C26–C28 tetraenes)/(label in [^3H]24:4) increased from 0.1 in PtSs to 2.5 in LSs. Simultaneously, the ratio (sum of [^3H]label in C26–C32 pentaenes)/(label in [^3H]24:5) increased from 0.25 in PtSs to 2.8 in LSs. From the data in Fig. 7, where comparable amounts of protein from isolated spermatogenic cells were used, it was clear that the PUFA elongation activity of *Elov4* during spermatogenesis tended to decline with the progression of cell differentiation in the direction PtS \rightarrow RS \rightarrow LS (Fig. 7). The fact that *Elov4* protein also decreased its levels in the order PtS \rightarrow RS, but then reappeared concentrated in LSs (Fig. 6), supports our interpretation that, although present, most of the enzyme existent in LSs was partially inactive.

Fa2h protein expression

In parallel to the reported age-related increase in the proportions of h-Vs in the SM and Cer of rat testis (4), *Fa2h* protein levels increased in this organ as its maturation proceeded (Fig. 8). With the antibody used, *Fa2h* was detected

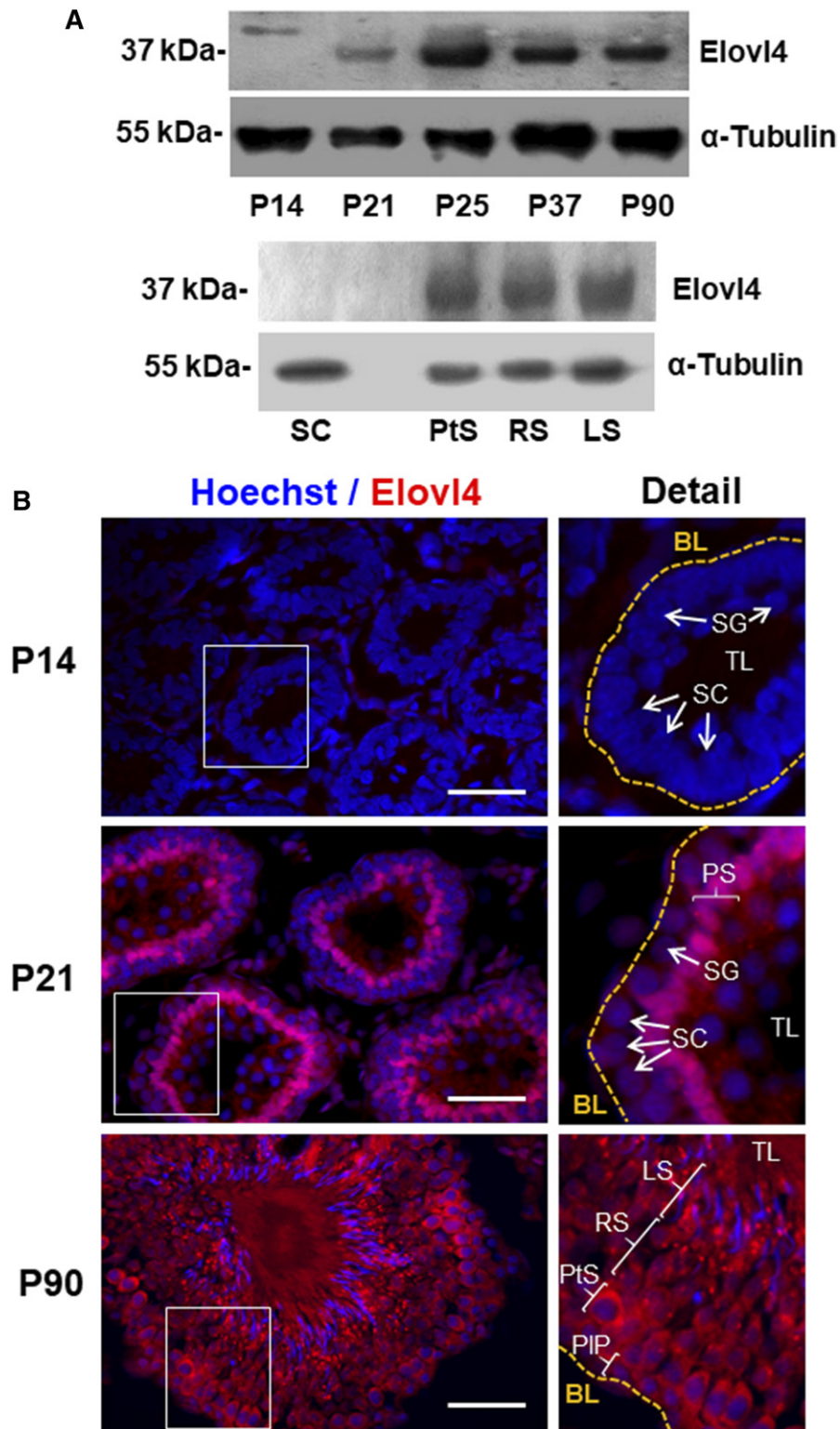


Fig. 5. Expression of the Elov14 protein in rat testes. A: Western blots of the protein at the indicated postnatal days, and in isolated cell populations from adult seminiferous epithelium. B: Immunolocalization of Elov14 (red) in the seminiferous epithelium at three postnatal ages (bars = 100 μ m). The squares in white delineate the enlarged details shown on the right. No Elov14-labeling was detected at P14 in the prepubertal seminiferous epithelium, rich in SCs and SG. At P21, the row of intensely stained cells corresponds to PtSs. Elov14-labeling remained in these cells and was also evident in postmeiotic spermatogenic cells (spermatids) from adult testis (P90, tubular stage VII–VIII). Basal lamina (BL, yellow dotted lines) and tubular lumen (TL) are indicated. PIP, preleptotene spermatocytes.

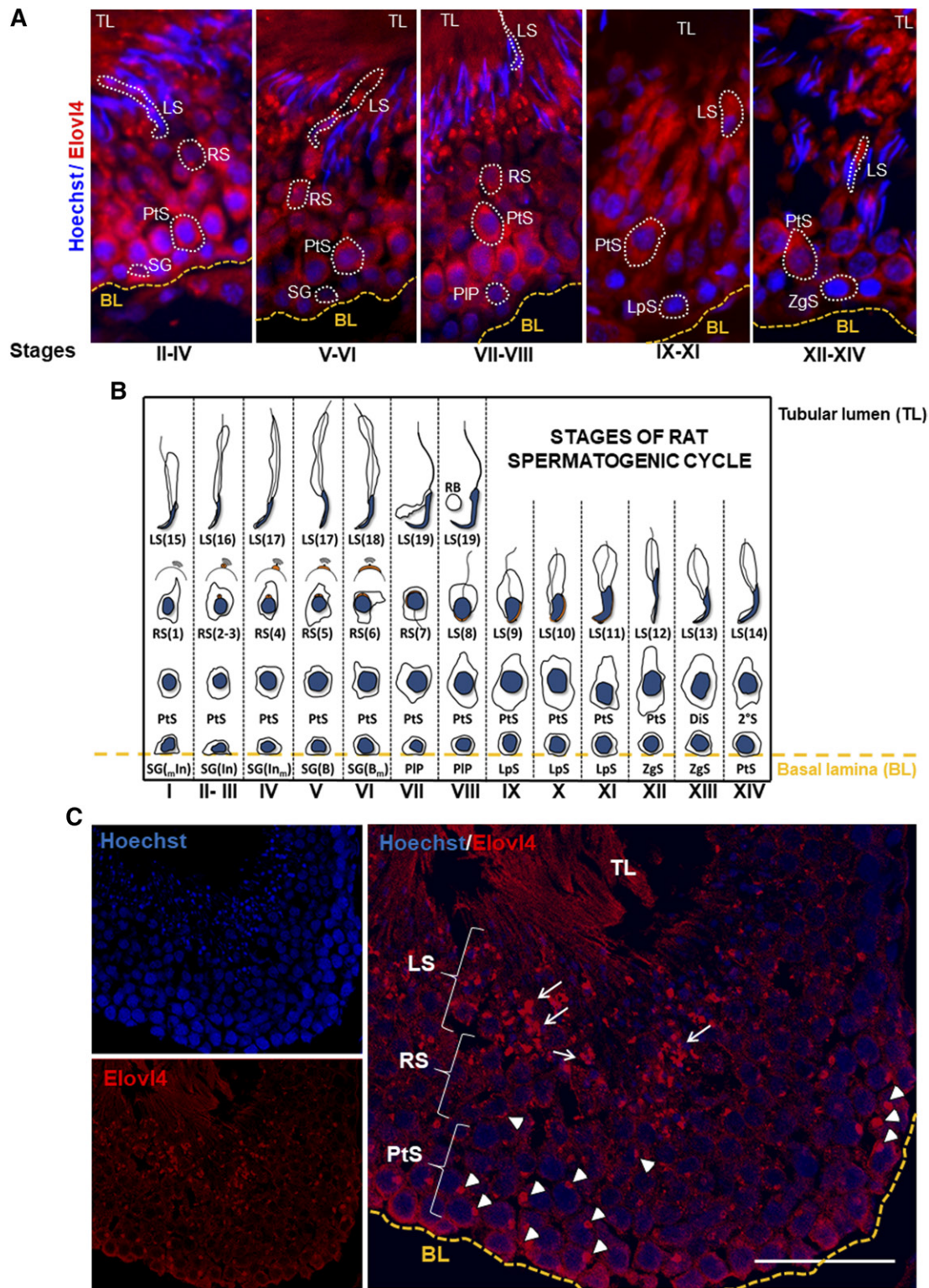


Fig. 6. A: Distribution of Elov14 in the adult testis at the indicated stages of the seminiferous epithelium cycle. The protein was strongly expressed in PSs, mainly PtSs, in a stage-dependent way. Their staining was the most intense among tubule cells at stages III–IV and VII–VIII, but was faint at stages V–VI, IX–XI, and XII–XIV. The protein level was even fainter in RSs and reappeared concentrated in small spot-like structures in elongating (early and late) spermatids (LS). B: Representative scheme of the rat spermatogenic cell differentiation cycle and the associated tubular stages, redrawn from material published by Russell et al. in 1983 (54). SGs (B, type B; In, intermediate; m, meiotic SGs); PIP, preleptotene spermatocytes; DiS, diplotene spermatocytes; LpS, leptotene spermatocytes; ZgS, zygotene spermatocytes; 2°S, secondary meiotic spermatocytes; RB, residual body. C: Confocal images (bar = 50 μ m). Elov14 localization was mostly perinuclear in PSs and RS (arrow heads). The protein, in an indeterminate cytoplasmic localization, appeared densely packed in LS (arrows). Basal lamina (BL, yellow dotted lines) and tubular lumen (TL) are indicated.

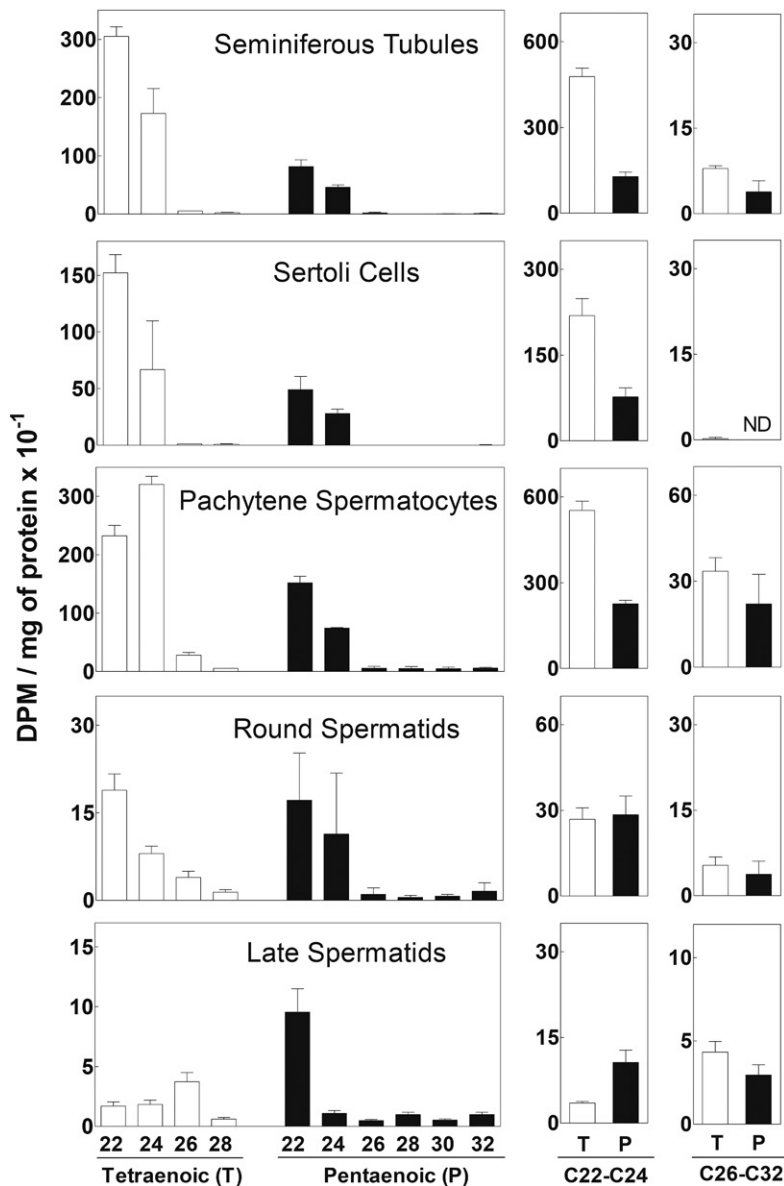


Fig. 7. Conversion of arachidonic acid into PUFAs with longer chains by cell populations from the adult rat seminiferous epithelium cells. Total STs, and the indicated cells isolated therefrom, were independently maintained for 20 h in culture with [^3H]20:4n-6 as a precursor. In each case the total lipid was extracted, its fatty acids were converted into methyl esters, the latter were separated into tetraenoic (T) and pentaenoic (P) fatty acid fractions, and their components were resolved by HPLC. To comparatively summarize the activity of Elov12 and Elov15 on the one hand, and that of Elov14 on the other, the sum of label in (T + P) C22–C24 and C26–C32 fatty acids, respectively, is shown in the right panels. ND, not detected.

faintly in Western blots before P25, when it showed a marked increase (Fig. 8A). This timing coincided with the start of the second meiotic division and emergence of the first haploid spermatids. The Fa2h protein levels reached their apparent maximum at P37, as they were similar from this age to adulthood.

Spermatogenic cells were the only cells in STs in which the Fa2h protein was expressed (Fig. 8B). Such expression was lower in spermatocytes than in spermatids, in agreement with the enrichment in h-V-containing SLs associated with the PtS \rightarrow RS progression (3).

In spermatids, Fa2h levels and intracellular location varied with the seminiferous epithelium stages. The protein reached its maximum level in LSs at stages III–IV, V–VI, IX–XI, and XII–XIV of the spermatogenic cycle. In spermatids at IX–XI stages, the protein was located in the cell cytoplasm, whereas in the other three stages it was concentrated in the posterior region of the heads, partially covering the cell chromatin-condensing nuclei. These three

spermatogenic stages contain spermatids undergoing the most advanced steps of spermiogenesis, up to steps 17 and 18. Over the curved heads of these spermatids, Fa2h was clearly observed to surround the nuclear envelope partially: its fluorescence was intensely focused over the posterior aspect (i.e., that pointing to the lumen) of the spermatid heads. The thin and slightly curved spermatid head apices (pointing backward into the epithelium) were uncovered, as indicated by the Hoechst blue staining of the spermatid nuclear chromatin protruding out from the fluorescent structure. Confocal imaging confirmed that, in these LSs, Fa2h was concentrated over the nuclear envelope (Fig. 8C, D), in a location that suggested coincidence with the structure known as “manchette,” a temporary cup-like formation that surrounds the spermatids head during their elongation. The high Fa2h concentration in this LS area was also transient. At spermatogenic stages VII–VIII, which contain spermatids at the step just preceding spermiation (step 19), Fa2h had totally disappeared (Fig. 8B),

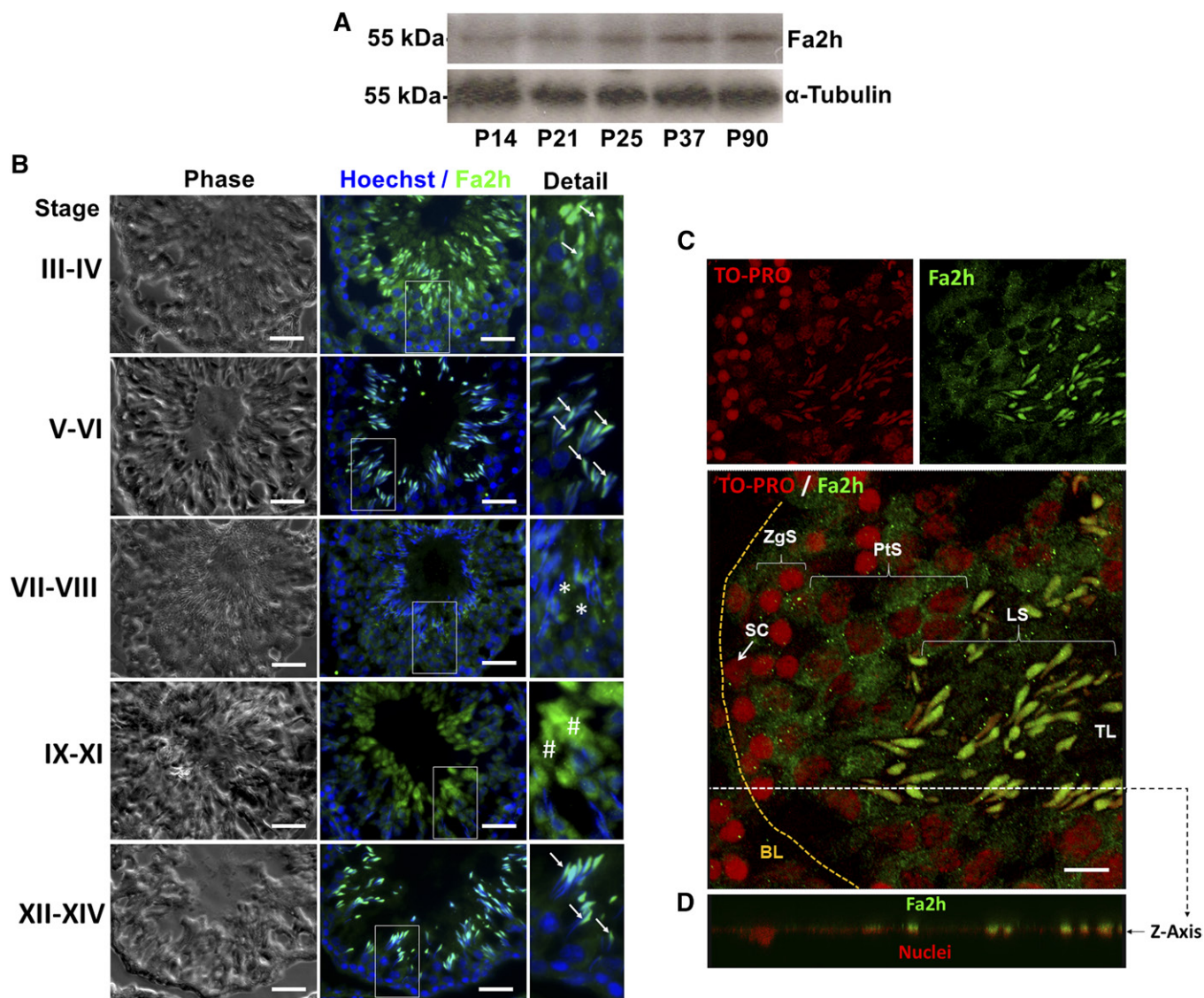


Fig. 8. Expression and localization of Fa2h in the rat seminiferous epithelium. **A:** Western blots showing the expression of Fa2h in testes at the indicated postnatal days. **B:** Stage-dependent expression of Fa2h in the adult seminiferous epithelium (bars = 50 μm), as revealed by immunofluorescence. The Fa2h protein was exclusively expressed in spermatids. It reached its maximum in LSs that were at the III–IV, V–VI, IX–XI, and XII–XIV stages of the spermatogenic cycle. Of these stages, the protein location was cytoplasmic (#) at IX–XI (steps 9–11), and in the rest of stages, which contain more advanced spermatids (up to steps 13–18 of spermiogenesis), it was concentrated around the highly condensed chromatin of the blue-stained cell nuclei (arrows). In later spermatids (stages VII–VIII, step 19 of spermiogenesis), Fa2h was no longer stained (*), indicating that its expression was temporary. **C:** Confocal microscopy to show the location of nuclei (TO-PRO, red) in comparison to Fa2h (green) at stages XII–XIV, using immunofluorescence (bar = 10 μm). Fa2h appeared concentrated close to the LSs' nuclei. The dashed cross-section line indicates the tissue section analyzed by orthogonal sectioning in the image below. Basal lamina (BL, yellow dashed lines) and tubular lumen (TL) are indicated. **D:** Section through the Z-axis showing that Fa2h rests in close apposition to the nuclear envelope of late (steps 13–16) spermatids.

for it was also absent from the free spermatozoa located in the tubule lumen.

DISCUSSION

In the present study, six of the seven members of the *Elovl* family are shown to be expressed in the adult rat testis. All of their mRNAs are produced by cells located within the STs, varying in levels among spermatogenic cells and most being also expressed in somatic SCs. Our analysis showed that *Elovl5*, *Elovl2*, and *Elovl4* are differentially expressed

during postnatal development, until relatively stable expression levels of each are reached in the adult testis, where the three transcripts are mostly contributed by spermatogenic cells.

Elovl5 and *Elovl2*

Elongation of diet-derived 18:2n-6 to C20–C22 PUFAs is mostly a function of *Elovl5*, while elongation of the latter to C24 PUFAs is mostly associated with *Elovl2*. These two elongases, but especially *Elovl2*, are regarded as rate-limiting in the production of the C24 PUFA acyl-CoAs (10). The

present quantitative comparisons showed that *Elovl5* mRNA is already expressed in rat testes at developmental ages at which *Elovl2* (and C20–C22 PUFA) levels are still very low, whereas *Elovl2* is strongly upregulated in parallel with the emergence of the C20-rich spermatocytes and C22-rich spermatids (3, 22, 41). Interestingly, in liver from *Elovl5*^{-/-} mice, *Elovl2* is upregulated, and the synthesis of C20 and C22 PUFAs is not interrupted (42). This reflects the partial overlapping between the activities of these two enzymes. In comparison, in testes of *Elovl2*^{-/-} mice, the deficiency of C22, and especially that of C24 PUFAs and longer polyenes like 30:5n-6, is not compensated (10), demonstrating the importance of *Elovl2* in providing the PUFAs that serve as substrates to *Elovl4*.

The high mRNA levels of *Elovl2* in spermatogenic cells, and the fact that PSs and early spermatids are the cells most susceptible to temperature in the adult testis (43) explains our present finding that *Elovl2* mRNA levels were the most reduced in the adult rat testis 2 weeks after the massive germ cell depletion induced by exposures to hyperthermia. In contrast, *Elovl5* mRNA levels had increased more than twice in the same 2 week period, indicating upregulation of this gene in the reemerging germ cells. These are the newly formed PtSs requiring the synthesis of the C20 PUFAs normally abundant in their membrane glycerophospholipids. A similar rising trend seems to have affected the *Elovl4* expression, which, by the same token, could respond to PtSs requiring the n-Vs that normally abound in their Cer and SM (3). The finding that, after their significant drops at week 2, *Elovl2* (and also *Fa2h*) mRNA levels tended to increase at week 6 posthyperthermia, coincides with the timing of reappearance in the testis of spermatids, concomitantly with their 22:5-rich glycerophospholipids and h-V-rich SLs.

Elovl4

As previously shown in the adult mouse (14), our work shows that *Elovl4* mRNA is actively produced in the adult rat testis. It goes on to demonstrate that such mRNA is differentially expressed among spermatogenic cells. In addition, of the three elongases compared here, *Elovl4* was the one whose mRNA levels were higher in SCs than in germ cells, an intriguing finding considering that the former somatic cells failed to express *Elovl4* protein and to produce C26–C32 PUFA. Conversely, in the n-V-rich PtSs (3), where the protein was highly concentrated and most active as an elongase, the mRNA levels were the lowest. Although the reasons for these features remain elusive at present, the high mRNA levels in SCs provided a reasonable explanation to our present in vivo observations in two situations in which SCs outnumber germ cells: the infantile gonads (not yet producing the latter) and the adult testes undergoing the consequences of hyperthermia (having lost most of them). In each of these cases, *Elovl4* mRNA transcripts were present because they were mainly contributed by SCs.

The transcriptionally expressed, but translationally silent, *Elovl4* mRNA in SCs suggests that it may be subject to negative regulation or silencing in these cells. If this were the case, however, the next question would be why SCs

should need to produce *Elovl4* mRNA. Extracellular microvesicles are part of the cell secretome, and carry proteins and functional RNA species (including mRNA, noncoding RNA, and miRNA) from one cell to another, where mRNAs may be translated into appropriate proteins (44). This horizontal transfer of RNA could potentially occur from SCs to spermatogenic cells, especially to PtSs. Small membrane-bound vesicles of endosomal origin, known as exosomes, are released by many cells, mediating intercellular transport of proteins, lipids, and RNAs (45, 46). Although not yet characterized in rat SCs, the presence of exosomes has been described in turtle testes (47).

Also intriguingly, we also detected significant *Elovl4* mRNA at embryonic ages in the primordial testes of the rat (unpublished observations), i.e., far from the moment in life in which membrane lipids that contain n-Vs are expected to arise. Small amounts of translated *Elovl4* enzyme should suffice to give rise to n-Vs that could be modified by other enzymes to synthesize products involved in regulatory functions. In this regard, a recent discovery in the mouse retina showed that two n-Vs from the retina, 32:6n-3 and 34:6n-3, in free form, can be converted by oxygenases into a novel series of compounds termed “elovanoids” (48). These molecules, formed in cells of the retinal pigment epithelium and released to the medium in nanomolar concentrations, were shown to enhance the expression of pro-survival genes in photoreceptors (48).

As a testicular protein, *Elovl4* was not detected in extratubular locations and it showed a differential spatiotemporal pattern of expression among germ cells. Meiotic spermatocytes intensely expressed *Elovl4* at specific spermatogenic cell stages and in a cell location that was compatible with its concentration in Golgi structures and in the ER. The protein staining decreased with differentiation between PtSs and RSs, as also did the ability to produce C26–C32 PUFAs from PtSs to RSs, suggesting that *Elovl4* was gradually less necessary as differentiation proceeded. This is reasonable, as an important part of the lipid materials synthesized in the large-sized PtSs, including the polar lipids of plasma membrane and intracellular organelles, are “inherited” by its two postmeiotic daughter RSs.

In spermatids at more advanced stages of differentiation, namely those subject to the steps of spermiogenesis, the *Elovl4* protein appeared concentrated in a small rounded structure within the cytoplasmic lobe. This formation may correspond to the “radial body” previously described in rat elongated spermatids, an aggregate of collapsed and radially arranged remnants of ER cisternae (49). The high *Elovl4* protein concentration detected by the antibody, together with the weakest elongation activity observed in LSs, suggest that the protein, active in the ER at earlier stages, eventually loses part of its functionality at the last stages of spermiogenesis. Its high concentration in the mentioned small round structures probably reflects the final destination of former ER membranes, together with other disposable organelles and extranuclear components, to the particles known as “residual bodies”. These small membrane-bound structures, destined to be phagocytized by SCs, are known to concentrate, in a highly compact


form, organelles and other intracellular materials no longer needed in the nascent gametes. This was apparently the fate of *Elovl4* and *Fa2h*, as both proteins were absent from testicular spermatozoa.

CerS3 is the member of the Cer synthase gene family that is specifically expressed in spermatogenic cells (6), where it is responsible for the synthesis of Cer species with VLCPUFAs (7, 50), thereby leading to SM and other VLCPUFA-containing SLs. The pattern of expression of *Elovl4* observed here among cells of rat STs coincided with that of the CerS3 protein described in mice by Rabionet et al. (7) in that both protein levels were highest in PtSs, declining in RSs, and concentrated again in small round structures present in LSs. Taken together, these results suggest that the expression of *Elovl4* and *CerS3*, at the mRNA and protein level, tend to precede that of *Fa2h* during spermatogenesis, and that these enzymes concertedly collaborate in the biosynthesis of the SLs with VLCPUFAs that are destined to spermatozoa.

Fa2h

Unlike *Elovl4* mRNA, the *Fa2h* mRNA expression was undetectable in SCs. Consistently, it was apparently absent from immature rat testis and it vanished from the adult rat testis when the loss of germ cells with permanence of SCs was experimentally forced as a consequence of repeated exposures to hyperthermia. Not surprisingly, the *Fa2h* expression, at the mRNA and protein levels, was highest in spermatids, where its products, h-Vs, tend to concentrate in Cer and SM species (3).

The most interesting finding about *Fa2h* protein was its spermatogenic stage-specific localization. Meager in PtSs, its staining appeared abundant and disseminated in the cytoplasm of RSs, as expected from the ER localization of *Fa2h* as an integral membrane protein (23, 51) and from the accretion of its h-V products in these cells (3). At late steps of spermiogenesis, the protein had evidently undergone a change in its position within cells, indicative of intracellular membrane transport. In the spermatids situated most distally from the limiting membrane of the tubules, the fluorescence associated to *Fa2h* was found to surround the nuclear envelope partially, intensely focused over the posterior aspect of the head of the elongating spermatids, in coincidence with the formation of the temporary structure known as manchette. The changes in shape that the heads of rat spermatids undergo during spermiogenesis, from roughly spherical to sickle-shaped, critically depend on this complex microtubule-based structure (52). Actin filaments, microtubules, and GM1-rich raft microdomains participate in allowing the correct assembly and anchoring of the manchette complex (53). The function of the enzymes, *Elovl4* and *Fa2h*, is evidently to work in partnership to produce germ cell membrane SLs with VLCPUFAs, which, unlike those with saturated fatty acids, occur in membrane regions distinctly apart from "raft-like" domains (22). The present observations suggest that the relationship between *Fa2h* and manchette functions may be simple coexistence and cooperation, the former facilitating, the latter operating the changes in head shape that take place

in LSs. The n-Vs, and especially the rodent-specific h-V-containing SLs, may provide the necessary flexibility to the membrane of spermatids as their heads increase their curvature, enabling the formation of the hook-shaped head that is typical of mouse and rat spermatozoa. 

The authors gratefully acknowledge Drs. Robert E. Anderson and Martin-Paul Agbaga (University of Oklahoma Health Sciences Center, Oklahoma City, OK) for kindly giving us the antibody against *Elovl4*.

REFERENCES

1. Robinson, B. S., D. W. Johnson, and A. Poulos. 1992. Novel molecular species of sphingomyelin containing 2-hydroxylated polyenoic very-long-chain fatty acids in mammalian testes and spermatozoa. *J. Biol. Chem.* **267**: 1746–1751.
2. Furland, N. E., S. R. Zanetti, G. M. Oresti, E. N. Maldonado, and M. I. Avelaño. 2007. Ceramides and sphingomyelins with high proportions of very long-chain polyunsaturated fatty acids in mammalian germ cells. *J. Biol. Chem.* **282**: 18141–18150.
3. Oresti, G. M., J. G. Reyes, J. M. Luquez, N. Osses, N. E. Furland, and M. I. Avelaño. 2010. Differentiation-related changes in lipid classes with long-chain and very long-chain polyenoic fatty acids in rat spermatogenic cells. *J. Lipid Res.* **51**: 2909–2921.
4. Zanetti, S. R., M. M. de Los Angeles, D. E. Rensetti, M. W. Fornes, and M. I. Avelaño. 2010. Ceramides with 2-hydroxylated, very long-chain polyenoic fatty acids in rodents: From testis to fertilization-competent spermatozoa. *Biochimie.* **92**: 1778–1786.
5. Sandhoff, R., R. Geyer, R. Jennemann, C. Paret, E. Kiss, T. Yamashita, K. Gorgas, T. P. Sijmonsma, M. Iwamori, C. Finaz, et al. 2005. Novel class of glycosphingolipids involved in male fertility. *J. Biol. Chem.* **280**: 27310–27318.
6. Rabionet, M., A. C. van der Spoel, C. C. Chuang, B. von Tumpling-Radosta, M. Litjens, D. Bouwmeester, C. C. Hellbusch, C. Korner, H. Wiegandt, K. Gorgas, et al. 2008. Male germ cells require polyenoic sphingolipids with complex glycosylation for completion of meiosis: a link to ceramide synthase-3. *J. Biol. Chem.* **283**: 13357–13369.
7. Rabionet, M., A. Bayerle, R. Jennemann, H. Heid, J. Fuchser, C. Marsching, S. Porubsky, C. Bolenz, F. Guillou, H. J. Grone, et al. 2015. Male meiotic cytokinesis requires ceramide synthase 3-dependent sphingolipids with unique membrane anchors. *Hum. Mol. Genet.* **24**: 4792–4808.
8. Jakobsson, A., R. Westerberg, and A. Jakobsson. 2006. Fatty acid elongases in mammals: their regulation and roles in metabolism. *Prog. Lipid Res.* **45**: 237–249.
9. Leonard, A. E., B. Kelder, E. G. Bobik, L. T. Chuang, C. J. Lewis, J. J. Kopchick, P. Mukerji, and Y. S. Huang. 2002. Identification and expression of mammalian long-chain PUFA elongation enzymes. *Lipids.* **37**: 733–740.
10. Zadravec, D., P. Tvrdik, H. Guillou, R. Haslam, T. Kobayashi, J. A. Napier, M. R. Capecchi, and A. Jakobsson. 2011. ELOVL2 controls the level of n-6 28:5 and 30:5 fatty acids in testis, a prerequisite for male fertility and sperm maturation in mice. *J. Lipid Res.* **52**: 245–255.
11. Avelaño, M. I. 1987. A novel group of very long chain polyenoic fatty acids in dipolyunsaturated phosphatidylcholines from vertebrate retina. *J. Biol. Chem.* **262**: 1172–1179.
12. Avelaño, M. I., and H. Sprecher. 1987. Very long chain (C24 to C36) polyenoic fatty acids of the n-3 and n-6 series in dipolyunsaturated phosphatidylcholines from bovine retina. *J. Biol. Chem.* **262**: 1180–1186.
13. Umeda, S., R. Ayyagari, M. T. Suzuki, F. Ono, F. Iwata, K. Fujiki, A. Kanai, Y. Takada, Y. Yoshikawa, Y. Tanaka, et al. 2003. Molecular cloning of ELOVL4 gene from cynomolgus monkey (*Macaca fascicularis*). *Exp. Anim.* **52**: 129–135.
14. Mandal, M. N., R. Ambasudhan, P. W. Wong, P. J. Gage, P. A. Sieving, and R. Ayyagari. 2004. Characterization of mouse orthologue of ELOVL4: genomic organization and spatial and temporal expression. *Genomics.* **83**: 626–635.
15. Zhang, X. M., Z. Yang, G. Karan, T. Hashimoto, W. Baehr, X. J. Yang, and K. Zhang. 2003. *Elovl4* mRNA distribution in the developing

- mouse retina and phylogenetic conservation of Elovl4 genes. *Mol. Vis.* **9**: 301–307.
16. Zhang, K., M. Kniazeva, M. Han, W. Li, Z. Yu, Z. Yang, Y. Li, M. L. Metzker, R. Allikmets, D. J. Zack, et al. 2001. A 5-bp deletion in ELOVL4 is associated with two related forms of autosomal dominant macular dystrophy. *Nat. Genet.* **27**: 89–93.
 17. Grayson, C., and R. S. Molday. 2005. Dominant negative mechanism underlies autosomal dominant Stargardt-like macular dystrophy linked to mutations in ELOVL4. *J. Biol. Chem.* **280**: 32521–32530.
 18. Vasireddy, V., P. Wong, and R. Ayyagari. 2010. Genetics and molecular pathology of Stargardt-like macular degeneration. *Prog. Retin. Eye Res.* **29**: 191–207.
 19. Barabas, P., A. Liu, W. Xing, C. K. Chen, Z. Tong, C. B. Watt, B. W. Jones, P. S. Bernstein, and D. Krizaj. 2013. Role of ELOVL4 and very long-chain polyunsaturated fatty acids in mouse models of Stargardt type 3 retinal degeneration. *Proc. Natl. Acad. Sci. USA.* **110**: 5181–5186.
 20. Agbaga, M. P., R. S. Brush, M. N. Mandal, K. Henry, M. H. Elliott, and R. E. Anderson. 2008. Role of Stargardt-3 macular dystrophy protein (ELOVL4) in the biosynthesis of very long chain fatty acids. *Proc. Natl. Acad. Sci. USA.* **105**: 12843–12848.
 21. Harkewicz, R., H. Du, Z. Tong, H. Alkuraya, M. Bedell, W. Sun, X. Wang, Y. H. Hsu, J. Esteve-Rudd, G. Hughes, et al. 2012. Essential role of ELOVL4 protein in very long chain fatty acid synthesis and retinal function. *J. Biol. Chem.* **287**: 11469–11480.
 22. Santiago Valtierra, F. X., M. V. Mateos, M. I. Aveldaño, and G. M. Oresti. 2017. Sphingomyelins and ceramides with VLCPUFAs are excluded from low-density raft-like domains in differentiating spermatogenic cells. *J. Lipid Res.* **58**: 529–542.
 23. Eckhardt, M., A. Yaghootfam, S. N. Fewou, I. Zoller, and V. Gieselmann. 2005. A mammalian fatty acid hydroxylase responsible for the formation of alpha-hydroxylated galactosylceramide in myelin. *Biochem. J.* **388**: 245–254.
 24. Alderson, N. L., E. N. Maldonado, M. J. Kern, N. R. Bhat, and H. Hama. 2006. FA2H-dependent fatty acid 2-hydroxylation in postnatal mouse brain. *J. Lipid Res.* **47**: 2772–2780.
 25. Maldonado, E. N., N. L. Alderson, P. V. Monje, P. M. Wood, and H. Hama. 2008. FA2H is responsible for the formation of 2-hydroxy galactolipids in peripheral nervous system myelin. *J. Lipid Res.* **49**: 153–161.
 26. Hamanaka, S., M. Hara, H. Nishio, F. Otsuka, A. Suzuki, and Y. Uchida. 2002. Human epidermal glucosylceramides are major precursors of stratum corneum ceramides. *J. Invest. Dermatol.* **119**: 416–423.
 27. Uchida, Y., H. Hama, N. L. Alderson, S. Douangpanya, Y. Wang, D. A. Crumrine, P. M. Elias, and W. M. Holleran. 2007. Fatty acid 2-hydroxylase, encoded by FA2H, accounts for differentiation-associated increase in 2-OH ceramides during keratinocyte differentiation. *J. Biol. Chem.* **282**: 13211–13219.
 28. Romrell, L. J., A. R. Bellve, and D. W. Fawcett. 1976. Separation of mouse spermatogenic cells by sedimentation velocity. A morphological characterization. *Dev. Biol.* **49**: 119–131.
 29. Reyes, J. G., A. Diaz, N. Osses, C. Opazo, and D. J. Benos. 1997. On stage single cell identification of rat spermatogenic cells. *Biol. Cell.* **89**: 53–66.
 30. Karl, A. F., and M. D. Griswold. 1990. Sertoli cells of the testis: preparation of cell cultures and effects of retinoids. *Methods Enzymol.* **190**: 71–75.
 31. Hellemans, J., G. Mortier, P. A. De, F. Speleman, and J. Vandesompele. 2007. qBase relative quantification framework and software for management and automated analysis of real-time quantitative PCR data. *Genome Biol.* **8**: R19.
 32. Vandesompele, J., P. K. De, F. Pattyn, B. Poppe, R. N. Van, P. A. De, and F. Speleman. 2002. Accurate normalization of real-time quantitative RT-PCR data by geometric averaging of multiple internal control genes. *Genome Biol.* **3**: RESEARCH0034.
 33. Furland, N. E., J. M. Luquez, G. M. Oresti, and M. I. Aveldaño. 2011. Mild testicular hyperthermia transiently increases lipid droplet accumulation and modifies sphingolipid and glycerophospholipid acyl chains in the rat testis. *Lipids.* **46**: 443–454.
 34. Laemmli, U. K. 1970. Cleavage of structural proteins during the assembly of the head of bacteriophage T4. *Nature.* **227**: 680–685.
 35. Bligh, E. G., and W. J. Dyer. 1959. A rapid method of total lipid extraction and purification. *Can. J. Biochem. Physiol.* **37**: 911–917.
 36. Christie, W. W. 1982. *Lipid Analysis*. Pergamon Press, Oxford, UK.
 37. Oresti, G. M., P. L. Ayuza Aresti, G. Gigola, L. E. Reyes, and M. I. Aveldaño. 2010. Sequential depletion of rat testicular lipids with long-chain and very long-chain polyenoic fatty acids after X-ray-induced interruption of spermatogenesis. *J. Lipid Res.* **51**: 2600–2610.
 38. Vallés, A. S., M. I. Aveldaño, and N. E. Furland. 2014. Altered lipid homeostasis in Sertoli cells stressed by mild hyperthermia. *PLoS One.* **9**: e91127.
 39. Gregory, M. K., R. A. Gibson, R. J. Cook-Johnson, L. G. Cleland, and M. J. James. 2011. Elongase reactions as control points in long-chain polyunsaturated fatty acid synthesis. *PLoS One.* **6**: e29662.
 40. Gregory, M. K., L. G. Cleland, and M. J. James. 2013. Molecular basis for differential elongation of omega-3 docosapentaenoic acid by the rat Elovl5 and Elovl2. *J. Lipid Res.* **54**: 2851–2857.
 41. Beckman, J. K., and J. G. Coniglio. 1979. A comparative study of the lipid composition of isolated rat Sertoli and germinal cells. *Lipids.* **14**: 262–267.
 42. Moon, Y. A., R. E. Hammer, and J. D. Horton. 2009. Deletion of ELOVL5 leads to fatty liver through activation of SREBP-1c in mice. *J. Lipid Res.* **50**: 412–423.
 43. Hikim, A. P., Y. Lue, C. M. Yamamoto, Y. Vera, S. Rodriguez, P. H. Yen, K. Soeng, C. Wang, and R. S. Swerdloff. 2003. Key apoptotic pathways for heat-induced programmed germ cell death in the testis. *Endocrinology.* **144**: 3167–3175.
 44. Ratajczak, M. Z., and J. Ratajczak. 2016. Horizontal transfer of RNA and proteins between cells by extracellular microvesicles: 14 years later. *Clin. Transl. Med.* **5**: 7.
 45. Valadi, H., K. Ekstrom, A. Bossios, M. Sjostrand, J. J. Lee, and J. O. Lotvall. 2007. Exosome-mediated transfer of mRNAs and microRNAs is a novel mechanism of genetic exchange between cells. *Nat. Cell Biol.* **9**: 654–659.
 46. Colombo, M., G. Raposo, and C. Thery. 2014. Biogenesis, secretion, and intercellular interactions of exosomes and other extracellular vesicles. *Annu. Rev. Cell Dev. Biol.* **30**: 255–289.
 47. Ahmed, N., H. Yufei, P. Yang, Y. W. Muhammad, Q. Zhang, T. Liu, C. Hong, H. Lisi, C. Xiaoya, and Q. Chen. 2016. Cytological study on Sertoli cells and their interactions with germ cells during annual reproductive cycle in turtle. *Ecol. Evol.* **6**: 4050–4064.
 48. Jun, B., P. K. Mukherjee, A. Asatryan, M. A. Kautzmann, J. Heap, W. C. Gordon, S. Bhattacharjee, R. Yang, N. A. Petasis, and N. G. Bazan. 2017. Elovanooids are novel cell-specific lipid mediators necessary for neuroprotective signaling for photoreceptor cell integrity. *Sci. Rep.* **7**: 5279.
 49. Clermont, Y., and A. Rambourg. 1978. Evolution of the endoplasmic reticulum during rat spermiogenesis. *Am. J. Anat.* **151**: 191–211.
 50. Mizutani, Y., A. Kihara, and Y. Igarashi. 2006. LASS3 (longevity assurance homologue 3) is a mainly testis-specific (dihydro)ceramide synthase with relatively broad substrate specificity. *Biochem. J.* **398**: 531–538.
 51. Alderson, N. L., B. M. Rembiesa, M. D. Walla, A. Bielawska, J. Bielawski, and H. Hama. 2004. The human FA2H gene encodes a fatty acid 2-hydroxylase. *J. Biol. Chem.* **279**: 48562–48568.
 52. Russell, L. D., J. A. Russell, G. R. MacGregor, and M. L. Meistrich. 1991. Linkage of manchette microtubules to the nuclear envelope and observations of the role of the manchette in nuclear shaping during spermiogenesis in rodents. *Am. J. Anat.* **192**: 97–120.
 53. Simón, L., A. K. Funes, M. A. Yapur, M. E. Cabrilla, M. A. Monclus, P. V. Boarelli, A. E. Vincenti, T. E. Saez Lancellotti, and M. W. Fornes. 2017. Manchette-acrosome disorders during spermiogenesis and low efficiency of seminiferous tubules in hypercholesterolemic rabbit model. *PLoS One.* **12**: e0172994.
 54. Russell, L. D., R. A. Ettlin, A. P. Sinha Hikim, and E. D. Clegg. 1990. *Histological and Histopathological Evaluation of the Testis*. Cache River Press, Clearwater, FL.